

# Multi-frequency VLBI observations of the lens system B0128+437

A. D. Biggs<sup>1</sup> and I. W. A. Browne<sup>2</sup>

<sup>1</sup> Joint Institute for VLBI in Europe, Postbus 2, 7990 AA Dwingeloo, The Netherlands

<sup>2</sup> University of Manchester, Jodrell Bank Observatory, Macclesfield, Cheshire SK11 9DL U.K.

**Abstract.** We present high-resolution VLBI observations of the gravitational lens system B0128+437 discovered as part of the CLASS survey. VLBA observations at 5 GHz of this four-image system show that the background source consists of three separate sub-components, potentially giving a very large number of constraints when constructing the lens model. However, the three sub-component morphology is only reproduced in three of the images, the fourth image looking significantly different to the others. At the same time, a model of the mass distribution in the lens derived from MERLIN 5-GHz observations cannot reproduce the orientation of the sub-components in another of the images. The reasons for these unusual discrepancies are discussed, especially in the light of more recent VLBA+Effelsberg observations at 8.4 and 2.3 GHz. We briefly discuss the ionospheric corrections that can now be applied to radio interferometric data.

## 1. Introduction

The gravitational lens system B0128+437 (Phillips et al. 2000) was discovered during the CLASS gravitational lens survey (Browne et al. 2001), one of 22 that have been identified to date. MERLIN maps (Fig. 1) reveal four lensed images of a background AGN in a characteristic “quad” pattern, this being enough to confirm the lensing hypothesis. The maximum separation between the images is only 539 mas which suggests that the lensing galaxy is of low mass. Optical follow-up has proved disappointing with the detection of only a very faint smudge at *I*-band with *HST*, although the source is clearly detected at *K*-band with UKIRT albeit at low resolution.

An additional aspect of this system is that the lensed source has a GPS spectrum, peaking at around 1 GHz. The work of Snellen et al. (2000) on GPS sources allows an estimation of the intrinsic angular size of the radio source ( $1 \leq \theta \leq 10$  mas). In modelling the system, the positions and flux ratios of the lensed images are best fit with a Singular Isothermal Ellipsoid (SIE) model for the lensing galaxy plus some external shear. The position of the lensing galaxy and the position angle of the external shear were free parameters in the modelling.

A standard part of the CLASS follow-up is to observe all lenses with the VLBA. This can prove necessary to confirm the lensing hypothesis, but also gives more accurate positions and leads to increased modelling constraints if the source is resolved. Here we present observations made with the VLBA and VLBA+Effelsberg at three frequencies, 2.3, 5 and 8.4 GHz (S, C and X bands respectively).

## 2. VLBA 5-GHz Observations

The original VLBI observations were undertaken as part of the standard CLASS follow-up on 2000 December 20.

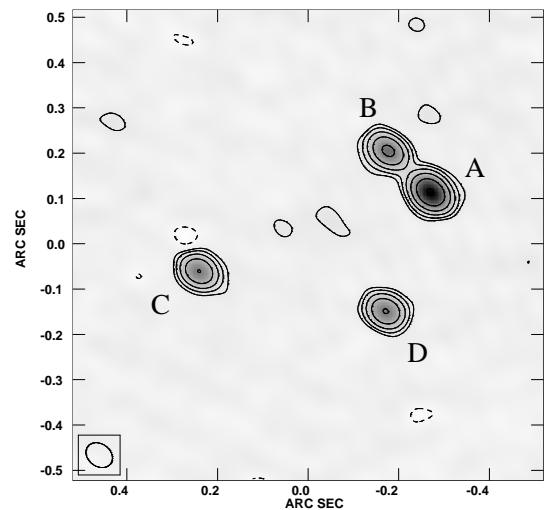
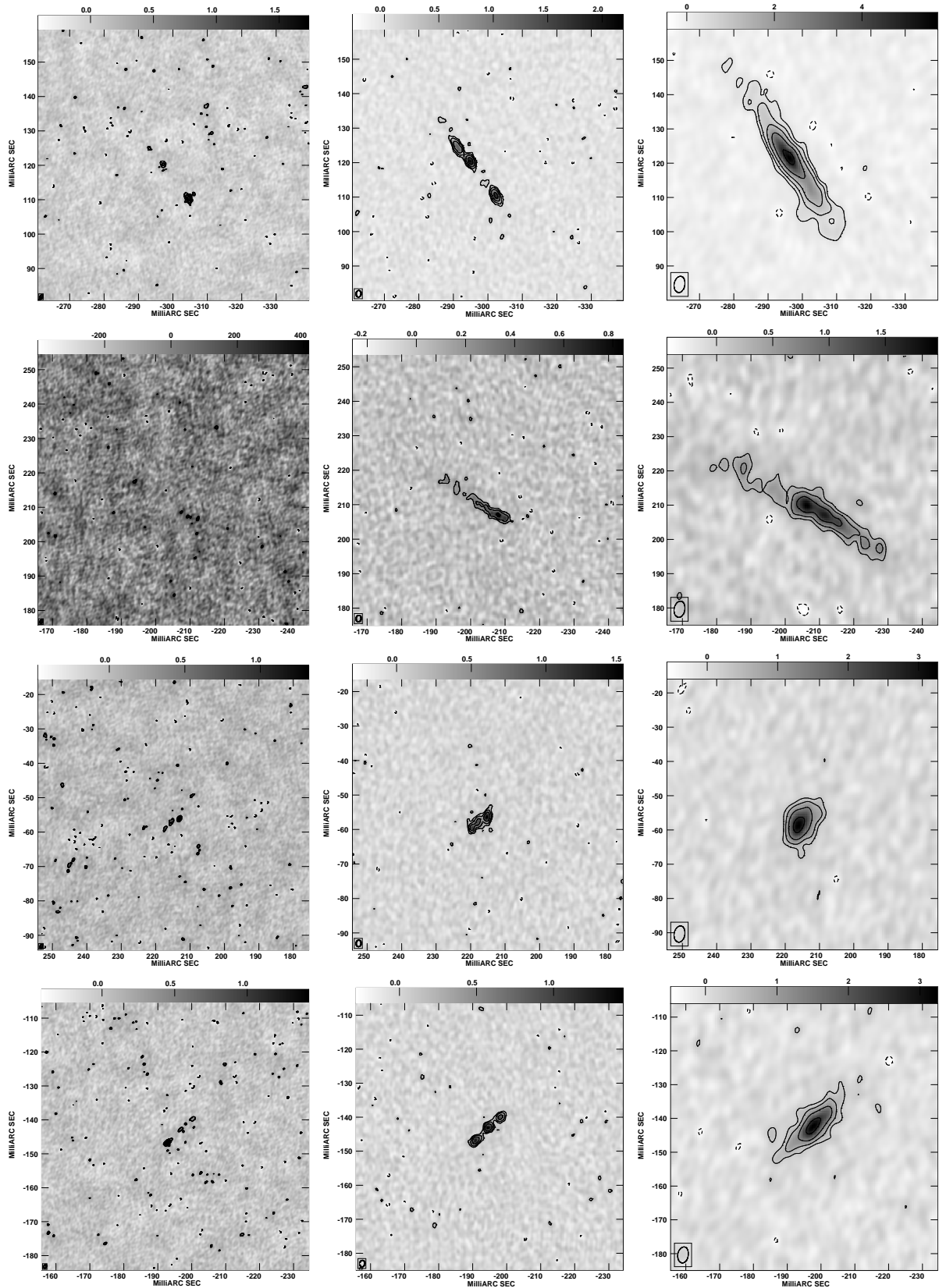


Fig. 1. MERLIN 5-GHz map of B0128+437.

These VLBA 5-GHz observations were phase-referenced with B0128+437 and the phase-reference source observed over a period of 13 hours. The maps made from these data can be seen in Fig. 2. The results look extremely promising in terms of the number of constraints for lens modelling. Three of the four images (A, C and D) consist of three distinct, but resolved, collinear sub-components. We are clearly seeing images of the same source, but with positions, sub-component shapes and flux ratios that have been distorted during the lensing. Model-fitting with elliptical Gaussians to each of these sub-components in DIFMAP or AIPS is fairly trivial and accounts for most of the flux in these images. Few lens systems rival B0128+437 in terms of this multiple discrete VLBI substructure. Other examples include the Double Quasar 0957+561



**Fig. 2.** Maps of B0128+437. Each row shows a different image with A at the top and D at the bottom. Each column shows a different frequency with 8.4 GHz at the left, 5 GHz in the middle and 2.3 GHz at the right. The 8.4-GHz data are naturally weighted whilst the other data are all weighted with a ROBUST value of zero. The grey scales represent surface brightness in units of  $\text{mJy beam}^{-1}$ , apart from the X-band map of image B where the units are  $\mu\text{Jy beam}^{-1}$ .

(Garrett et al. 1994) and MG 0414+0534 (Trotter, Winn & Hewitt 2000).

It is obvious, though, that image B does not look like the other images; it is far more diffuse and does not appear to have a three sub-component structure. Firstly, as it cannot be easily model-fitted this image is not very useful when it comes to lens modelling. Secondly, the A/B flux ratio from the MERLIN data is 2.0 and so, as lensing conserves surface brightness, we would expect image B to be half the size of image A. This would suggest that instead of the diffuse structures we observe with the VLBA at 5 GHz we should, if anything, be observing structures that are *more* point-like than in image A.

The conclusion we draw is that, in order for image B to be additionally distorted independently of the other images, it must be subject to some kind of propagation effect, most probably occurring in the lensing galaxy. Many lensed images are known to be strongly affected by the ionised interstellar media (ISM) of their lensing galaxies, a good example being the lens system JVAS B0218+357 (Patnaik et al. 1993). For instance, the polarisation position angle of the radio cores rotates with a  $\lambda^2$ -dependence as expected for Faraday rotation and both gradually depolarise at lower frequencies. It has been suggested that the south-west component in PKS 1830-211 is scatter-broadened in the ISM of the lensing galaxy (Guirado et al. 1999).

### 3. VLBA+Effelsberg S/X-band Observations

In order to further investigate this system, and the cause of the image B distortion in particular, further observations were taken with the VLBA at dual S/X-band. By examining the frequency-dependence of the structures it is hoped that the astrophysical effect at work can be identified. These observations took place on 2002 January 2 and included the 100-m telescope at Effelsberg in order to increase the resolution at S-band, thus aiding comparison with the existing C-band data, as well as to increase the image sensitivity at X-band where due to the source's GPS spectrum the images are very weak. As at C-band the observations were phase-referenced and both epochs used the same calibrator.

The results from the second epoch's data are also shown in Fig. 2. At X-band the images look very similar to those at C-band and are still dominated by three discrete sub-components. However, these observations in themselves are useful for lens modelling as they allow the individual sub-components in images A, C and D to be matched. Notice that whilst at C-band each sub-component is of comparable brightness, at X-band one sub-component in each is considerably brighter than the other two. Therefore the source has one sub-component with a flatter radio spectrum and we tentatively identify this as the core.

The new data do shed some light on image B. At X-band there is only the barest of detections and you may have to strain your eyes to see the few spots of emission on the map in Fig. 2! Clearly, the structure that we see

in the other images has not been recovered and so the effect does not seem to reduce at higher frequencies i.e. scatter-broadening would appear an unlikely explanation. At S-band, however, we find that image B now bears a striking resemblance to image A; the northern half of image A seems to correspond to the western half of image B. These S-band data therefore greatly clarify the situation regarding image B. At the other ends of these images though, differences are still apparent as the surface brightness of image B fades away to almost nothing, before perhaps recovering at its eastern extremity. This gives the impression of a hole in the jet. Furthermore, the area at which this hole lies is where we should expect to see the flat-spectrum sub-component that is identified in the other images.

An intriguing possibility is that the observed distortion of image B could be the result of a halo of black holes in the lens galaxy. This possibility has been explored by Wambsganss & Paczyński (1992) who show simulations of the radio jets of 0957+561 when perturbed by a halo of  $10^6 M_{\odot}$  black holes — milli-lensing. Their maps show various distortions of the intrinsic jet structure, including holes such as that we see in B0128+437. In addition we mention that the lens model is currently unable to explain the position angle of the sub-components in image C, which is offset from the model position angle by  $\sim 40^{\circ}$ . The work of Wambsganss & Paczyński also shows that jets can undergo such rotations as a result of milli-lensing.

### 4. Ionospheric correction

In this section we would now like to digress and turn to the topic of ionospheric corrections and their impact on VLBI data. Within AIPS a task called TECOR can remove the effects of the ionosphere from visibility data. It does this using files<sup>1</sup> of the total electron content (TEC) of the atmosphere that are constructed using dual-frequency signals broadcast by the GPS satellites. The VLBA have recently been encouraging their users to regard this task, which has been found to give useful corrections to data at frequencies as high as 8.4 GHz, as a routine part of their data reduction.

The effect of the ionosphere is to introduce an additional delay that scales as  $\nu^{-2}$  and which, due to the differing ionospheres over the widely-separated antennas in a VLBI array, can add many turns to the visibility phase and cause rapid phase-wrapping. This can seriously degrade the effectiveness of phase-referencing and for weak sources that cannot be self-calibrated, the goals of the experiment can be ruined. Experiments that are most affected are generally those that are observed during daylight and at low frequencies. Over the past two years or so the problem has been made much worse by the peak in the 11-year cycle of solar activity. The sun is still rather close

<sup>1</sup> down-loadable from NASA's Crustal Dynamics Data Interchange System (CDDIS) via anonymous ftp to: [cddis.gsfc.nasa.gov](http://cddis.gsfc.nasa.gov).

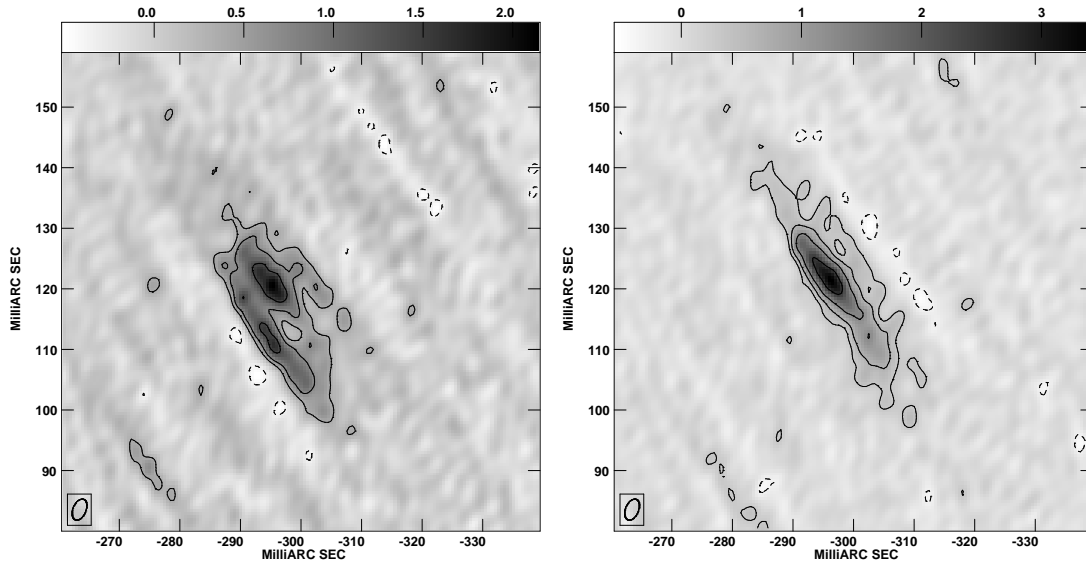


**Fig. 3.** Maps of image A of B0128+437 made immediately after SPLIT. Left is a map made without a correction for the ionosphere whilst on the right a correction has been applied as calculated using the TECOR task in AIPS.

to its maximum, although it will become increasingly less active in the next few years, and so this task can still be highly relevant for current as well as archival observations.

In Fig. 3 we show two maps of image A of B0128+437 made from the S-band data. The first map (on the left) is made without a correction for the atmosphere whilst in the map on the right TECOR has been run prior to fringe fitting. The results are impressive. Without the correction the image is extremely distorted whilst in the second map we do recover the true source structure. Whilst this experiment may not have been unrecoverable without the use of TECOR, the savings in time and mental expenditure are considerable. These observations were made with a phase-referencing cycle time of only 210 s and used a phase-reference source that was only one-third of a degree away from the target source. Even under these very favourable conditions, handicapped somewhat by the fact that the data were observed predominantly during daylight hours, the phase-referencing runs into severe difficulties without the ionospheric correction.

## 5. Conclusions

B0128+437 is an intriguing lens system. Before VLBI maps were available the system was believed to be rather unremarkable, with a model that could accurately reproduce the image positions and flux ratios. Now though we are faced with structures on mas-scales that cannot be explained with any simple lens model. The distortion of image B appears to be due to a propagation effect — a halo of black holes in the lensing galaxy is a possibility. This might explain the differences between this image and the others and also explain why the model cannot reproduce the orientation of the sub-components in image C.

Future work will need to make progress on our optical knowledge of this system which is sparse at the moment.

The current *HST* WFPC2 data show only a very faint blur which we assume is the lensing galaxy; there is no sign of any of the lensed images. The UKIRT *K*-band image on the other hand shows a much more convincing detection of the system and with a brightness distribution that appears to be dominated by the lensed images. This suggests that the lens galaxy contains a lot of dust. It seems therefore that future observations should concentrate on the infrared, maybe with the newly revived NICMOS camera on-board *HST*.

Finally, we note that this system is unlikely to be of much use for measuring  $H_0$  due to the GPS nature of the background source. These sources vary little in flux density and so measuring a time delay will prove impossible.

*Acknowledgements.* The VLBA and VLA are operated by the National Radio Astronomy Observatory which is a facility of the National Science Foundation operated under cooperative agreement by Associated Universities, Inc. A.D.B. acknowledges partial support from the EC ICN RadioNET (Contract No. HPRI-CT-1999-40003).

## References

- Browne I. W. A., et al., 2001, in ASP Conf. Ser. 237, Gravitational Lensing: Recent Progress and Future Goals, eds. T. G. Brainerd & C. S. Kochanek, 15
- Garrett M. A., Calder R. J., Porcas R. W., King L. J., Walsh D., Wilkinson P. N., 1994, MNRAS, 270, 457
- Guirado J. C., Jones D. L., Lara L., Marcaide J. M., Preston R. A., Rao A. P., Sherwood W. A., 1999, A&A, 346, 392
- Phillips P. M., et al., 2000, MNRAS, 319, L7
- Patnaik A. R., Browne I. W. A., King L. J., Muxlow T. W. B., Walsh D., Wilkinson P. N., 1993, MNRAS, 261, 435
- Trotter C. S., Winn J. N., Hewitt J. N., 2000, ApJ, 535, 671
- Wambsganss J., Paczyński B., 1992, ApJ, 397, L1